Acta Crystallographica Section B
Structural Science
ISSN 0108-7681

Geikielite–ecandrewsite solid solutions: synthesis and crystal structures of the $Mg_{1-x}Zn_xTiO_3$ ($0 \leq x \leq 0.8$) series

Ruslan P. Liferovich‡ and Roger H. Mitchell*

Department of Geology, Lakehead University, 955 Oliver Road, Thunder Bay, Ontario, Canada P7B 5E1

‡ Permanent address: Geological Institute KSC RAS, 14 Fersmana Str., Apatity 184200, Russia.

Correspondence e-mail: rmitchel@lakeheadu.ca

Received 16 June 2004
Accepted 21 July 2004

The crystal structures of members of the geikielite–ecandrewsite solid solution series, $Mg_{1-x}Zn_xTiO_3$ ($0 \leq x \leq 0.8$ a.p.f.u. Zn; a.p.f.u. = atoms per formula unit), synthesized by ceramic methods in air at ambient pressure, have been characterized by Rietveld analysis of X-ray powder diffraction patterns. These synthetic titanates adopt an ordered $R\overline{3}$ structure similar to that of ilmenite. The maximum solubility of Zn in $MgTiO_3$ is considered to be $\sim$ 0.8 a.p.f.u. Zn, as compounds with greater Zn content could not be synthesized at ambient conditions. Data are given for the cell dimensions and atomic coordinates, together with bond lengths, volumes and distortion indices for all the coordination polyhedra. Within the solid-solution series unit-cell parameters and unit-cell volumes increase with Zn content. All compounds consist of distorted $(Mg,Zn)O_6$ and TiO_6 polyhedra and, in common with geikielite and ilmenite (*sensu lato*), TiO_6 polyhedra are distorted to a greater extent than $(Mg,Zn)O_6$. The displacements of (Mg,Zn) and Ti from the centers of their coordination polyhedra vary insignificantly with increasing Zn content. The interlayer distance across the vacant octahedral site in the TiO_6 layer decreases slightly with the entry of the larger Zn^{2+} cation into the ^{vi}A site. The empirically obtained upper limit of the Goldschmidt tolerance factor (t) for $A^{2+}BO_3$ compounds adopting an ordered $R\overline{3}$ structure is 0.755. The absence of natural solid solutions between geikielite and ecandrewsite seems to be due to the contrasting geochemistry of Mg and Zn rather than for crystallochemical reasons.

1. Introduction

Ordered rhombohedral titanates, $A^{2+}TiO_3$, with the first-row transitional metals occupying the A site, are ilmenite-group compounds. The Fe-, Mn-, Mg- and Zn-dominated natural species are ilmenite (*sensu stricto*), pyrophanite, geikielite and ecandrewsite, respectively. These minerals are common accessories in a wide variety of igneous and metamorphic rocks. Geikielite is an important accessory in kimberlites and lamproites, and commonly forms in skarns developed after dolostones. Ecandrewsite is known from peralkaline rocks and their postmagmatic derivatives (Suwa *et al.*, 1987; Nakashima & Imaoka, 1998), low-to-middle grade metamorphic rocks, and hydrothermal parageneses comprising polymetallic ore deposits (Birch *et al.*, 1988; Whitney *et al.*, 1993).

Compositional data and crystallochemical characteristics are scarce for these titanates. The ilmenite–ecandrewsite ($Fe^{2+}_{1-x}Zn_xTiO_3$), pyrophanite–ecandrewsite ($Mn_{1-x}Zn_xTiO_3$) and ilmenite-pyrophanite ($Fe_{1-x}Mn_xTiO_3$) extended

© 2004 International Union of Crystallography
Printed in Great Britain – all rights reserved

solid solutions are known to exist in nature (Plimer, 1990; Mitchell & Liferovich, 2004*a*; Whitney *et al.*, 1993, respectively). Of these, the crystal structures of only the $Mn_{1-x}Zn_xTiO_3$ series have been characterized in detail on the basis of synthetic analogs (Mitchell & Liferovich, 2004*b*). A reconnaissance study also demonstrated the stability of solid solutions in the $Mg_{1-x}Mn_xTiO_3$ and $Mg_{1-2x}Zn_xMn_xTiO_3$ series, which have not been described in natural samples (Liferovich & Mitchell, 2004). As $^{vi}R_{Mg^{2+}} \simeq {}^{vi}R_{Zn^{2+}} < {}^{vi}R_{Fe^{2+}} < {}^{vi}R_{Mn^{2+}}$ [0.72, 0.74, 0.78 and 0.83 Å, respectively (Shannon, 1976)]; the absence of natural solid solutions between ecandrewsite, geikielite and/or pyrophanite seems to be due primarily to the differing geochemistries of Mg^{2+}, Fe^{2+}, Mn^{2+} and Zn^{2+} rather than for crystallochemical reasons (Liferovich & Mitchell, 2004).

The *ilmenite* structure is an ordered derivative of the *aristotype* corundum structure. Typically, the ilmenite structure is adopted by $A^{2+}Ti^{4+}O_3$ compounds when $^{vi}R_A \simeq {}^{vi}R_{Ti}$ and $^{vi}R_A << R_{O^{2-}}$, resulting in a Goldshmidt tolerance factor [*t* (Goldschmidt, 1926)] close to 0.75 (Mitchell, 2002). The ilmenite structure is based on *h.c.p.* (hexagonal closest packing) oxygen layers with cations occupying two thirds of the octahedral sites available. In contrast to the fully disordered corundum structure (space group $R\bar{3}c$), the ilmenite structure results from equal amounts of di- and tetravalent cations, which are ordered at the octahedral sites and alternate along the *c* axis of the unit cell. A pair of AO_6 and TiO_6 octahedra share a (001) face; each octahedron in the ilmenite structure shares an edge with the same type of octahedron and three edges with the other octahedra (Fig. 1*a*). The stacking sequence of cations along $[001]_h$ of this structure is '*A*-Ti-[]-Ti-*A*-[]' and 'Ti-Ti-[]' or '*A*-*A*-[]' parallel to (0001), resulting in a centrosymmetric $R\bar{3}$ rhombohedral cell.

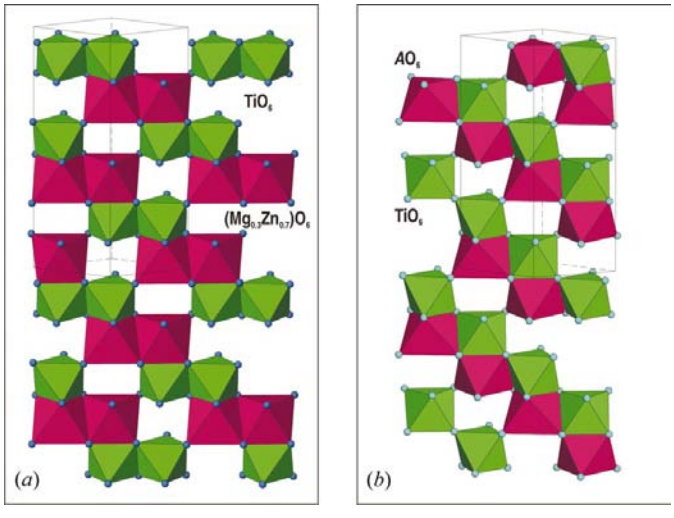

Figure 1
Projections onto the $(21\bar{1}0)$ plane of portions of the structures of: (*a*) $R\bar{3}$-structured synthetic $Mg_{0.3}Zn_{0.7}TiO_3$, obtained in the present study; (*b*) a high-pressure *R*3*c*-structured $A^{2+}TiO_3$ which is isostructural with $LiNbO_3$ (data adopted for $MnTiO_3$ from Ko & Prewitt 1988), illustrating the ordering and disposition of the face- and corner-sharing octahedra.

As in corundum, cations in the $R\bar{3}$ structure are displaced from the centers of both types of octahedra, resulting in the distortion of the coordination polyhedra. Various styles of distortion are known for ilmenite-structured compounds. The AO_6 polyhedron can be more distorted than the BO_6 polyhedron or *vice versa*, *e.g.* in ilmenite (*sensu stricto*) distortion of the TiO_6 octahedron is significantly higher than that of the FeO_6 octahedron (Mitchell, 2002). As both cation sites lie on threefold axes, each one has a single variable atomic positional parameter, *z*. Deviations of *z* from 1/3 and 1/6 for the *A* and Ti cations, respectively, are indicative of 'puckering' of the cation layers above and below the planes parallel to (001) (Wechsler & Prewitt, 1984).

Further structural distortion of the $A^{2+}Ti^{4+}O_3$ compounds can be driven by an increase in intensive parameters (*P* and/or *T*). The distortion can result in a phase transition to a structure with the '*A*-Ti-[]-*A*-Ti-[]' stacking sequence, both along and orthogonal to $[001]_h$ with the A^{2+} and Ti^{4+} cations occupying alternating layers. The structure has an *R*3*c* rhombohedral cell and is referred to as the lithium niobate ($LiNbO_3$) structure. This structure differs in the mode of connection of octahedra from that occurring in the ilmenite structure (Fig. 1*b*).

With a further increase in pressure, ilmenite- and Li-niobate-structured $ATiO_3$ compounds can undergo a phase transition to *Pbnm*-structured perovskite which is isostructural with the gadolinium orthoferrite ($GdFeO_3$; Linton *et al.*, 1999). Phase transformations between the ilmenite, lithium niobate and perovskite structures are complex and their study is hindered by kinetic factors and hysteresis effects (Mitchell, 2002).

Geikielite ($MgTiO_3$) is isostructural with ilmenite ($FeTiO_3$) at ambient pressure, but at high pressure it undergoes a phase transition to the Li-niobate structure as do $MnTiO_3$ and $FeTiO_3$ titanates (Linton *et al.*, 1999; Syono *et al.*, 1969; Ko & Prewitt, 1988). The only single-crystal structure study of natural ecandrewsite is that of the holotype with the composition $Zn_{0.59}Fe_{0.24}Mn_{0.17}TiO_3$ (Gatehouse & Nesbit, 1978). This mineral was found to be isostructural with ilmenite (Birch *et al.*, 1988). The space group of the synthetic $ZnTiO_3$ end-member is given as $R\bar{3}$ under ambient conditions (Bartram & Slepetys, 1961) and as *R*3*c* under unspecified conditions [JCPDS Powder Diffraction File Card No. 26-1500 ($ZnTiO_3$): Joint Committee for Powder Diffraction Standards, Sharthmore, PA (now ICDD)]. The former is very poorly defined ($R_{Bragg} = 0.135$) and the latter is not specified in terms of the *PT* parameters of the synthesis. Our experimental studies show that pure $ZnTiO_3$ cannot be formed in air by ceramic synthesis methods at ambient pressure over the temperature range 973–1573 K. Consequently, we were unable to determine the unit-cell dimensions and space group actually adopted by the $ZnTiO_3$ end-member. Owing to the poor quality of the data given by Bartram & Slepetys (1961), we consider the crystal structure of $ZnTiO_3$ to be not well established and is thus not considered further in the discussion below.

This contribution is part of an ongoing study of the crystallochemistry of complex ABO_3 oxides. The present research

Table 1
Refinement parameters and crystallographic characteristics of synthetic $(Mg_{1-x}Zn_x)TiO_3$ ($0 \leq x \leq 08$) at ambient conditions.

x	0	0.1	0.2	0.3	0.4	0.5	0.6	0.7	0.8
$^{vi}R_A^{2+}$ (Å)	0.72	0.73	0.73	0.73	0.73	0.73	0.73	0.73	0.74
t†	0.748	0.748	0.749	0.750	0.750	0.751	0.752	0.753	0.755
Phase composition									
ATiO$_3$ (%)	≥ 95	≥ 95	≥ 95	≥ 95	≥ 95	97.07	98.60	99.22	99.88
Other (%)	Arm	Arm, Ru	Arm, Ru	Arm, Ru	Arm, Ru	Ru 2.93	Ru (1.40)	Ru (0.78)	Ru (0.22)
Agreement factors									
R_{wp}	0.1337	0.1281	0.1268	0.1203	0.1143	0.1127	0.1118	0.1204	0.1126
R_{Bragg}	0.04570	0.02131	0.02139	0.01951	0.02342	0.02427	0.01571	0.02161	0.2264
GOF	1.60	1.57	1.54	1.55	1.51	1.48	1.55	1.61	1.58
DW	0.95	1.04	1.00	1.02	1.06	1.06	1.05	0.92	0.94
Unit-cell parameters									
a (Å)	5.05669 (4)	5.05758 (4)	5.05968 (3)	5.06232 (4)	5.06422 (4)	5.06690 (3)	5.06893 (4)	5.07109 (3)	5.07191 (4)
c (Å)	13.9034 (2)	13.9067 (1)	13.9114 (1)	13.9158 (1)	13.9182 (1)	13.9216 (1)	13.9232 (1)	13.9235 (1)	13.9243 (2)
c/a	2.750	2.750	2.749	2.749	2.748	2.748	2.747	2.746	2.745
V (Å^3)	307.883 (6)	308.064 (5)	308.422 (4)	308.844 (6)	309.127 (6)	309.532 (5)	309.814 (6)	310.085 (4)	310.204 (6)
Coordination polyhedra characteristics									
$\langle A-O1\rangle$ (Å)	2.088 (3)	2.113 (3)	2.114 (3)	2.119 (3)	2.124 (3)	2.126 (3)	2.130 (4)	2.138 (5)	2.156 (6)
V_{AO6} (Å^3)	11.644 (4)	12.062 (4)	12.062 (4)	12.120 (4)	12.183 (4)	12.206 (5)	12.245 (5)	12.392 (6)	12.694 (7)
A-shift (Å)	0.158	0.134	0.151	0.161	0.176	0.182	0.178	0.180	0.176
Δ_{AO6}	1.838	1.311	1.694	1.906	2.238	2.415	2.293	2.342	2.261
δ_{AO6}	75.62	75.95	79.87	83.52	88.11	89.37	92.95	93.14	93.47
$\langle$Ti$-$O1$\rangle$ (Å)	2.005 (3)	1.980 (3)	1.982 (3)	1.981 (3)	1.979 (3)	1.979 (4)	1.975 (4)	1.970 (5)	1.955 (6)
V_{TiO6} (Å^3)	10.394 (3)	9.975 (4)	9.993 (4)	9.986 (4)	9.971 (4)	9.973 (4)	9.906 (4)	9.826 (5)	9.582 (6)
Ti-shift (Å)	0.206	0.213	0.209	0.212	0.212	0.206	0.195	0.207	0.219
Δ_{TiO6}	3.405	3.641	3.457	3.580	3.555	3.377	3.017	3.408	3.734
δ_{TiO6}	61.74	69.06	70.04	68.78	65.72	65.71	67.62	68.09	72.82

† The tolerance factor for ABO_3 compounds is $t = (R_O + R_A)/[2^{1/2}(R_O + R_B)]$ (Goldschmidt, 1926). Arm armalcolite, Ru rutile.

was undertaken to determine the limits of solid solution between Mg and Zn in ilmenite-structured titanates and to investigate the response of the ordered $R\overline{3}$ structure to the replacement of Mg^{2+} by the slightly larger Zn^{2+} cation at critical values of the Goldschmidt tolerance factor, approaching and slightly exceeding $t = 0.75$ (Table 1). This is the first systematic study of the $Mg_{1-x}Zn_xTiO_3$ solid solution adopting the $R\overline{3}$ ilmenite structure.

2. Experimental and analytical methods

Mg–Zn titanates were synthesized from stoichiometric amounts of high-purity grade MgO, ZnO and TiO_2 (all from Aldrich Chemical Co.) by solid-state ceramic techniques. The reagents, dried at 293 K for several days, were mixed, ground in an agate mortar under acetone and calcined in air for 24 h at 1173 K. After regrinding, the samples were pressed into pellets at a pressure of 10 tonnes per cm^2 and then sintered in air for 48 h at 1273 K with careful regrinding after the first 24 h of the synthesis. The $MgTiO_3$ end-member did not form at 1273 K and was prepared at 1473 K. Thus, $T = 1273$ K was chosen for the synthesis of the $Mg_{1-x}Zn_xTiO_3$ series as a compromise between the temperature of synthesis of the $MgTiO_3$ end-member and $T = 1218$ K, which has been described as the upper limit of stability of the $ZnTiO_3$ end-member at ambient pressure (Kim *et al.*, 2001, and references therein).

The homogeneity and the compositions of all the titanates formed were assessed using a Jeol JSM-5900 scanning electron microscope (SEM) by back-scattered electron imagery (BSE) and quantitative X-ray energy-dispersive analysis (EDS). Step-scanned powder X-ray diffraction (XRD) patterns of the products were obtained at room temperature using a Philips 3710 diffractometer ($T = 293$ K; radiation Cu $K\alpha$; 2θ range 283–393 K, $\Delta 2\theta$ step 0.02°; counting time per step 4 s; graphite monochromator) with APD powder diffraction software.

XRD patterns were inspected using the Bruker AXS software package EVA to identify the phases present and confirm that $R\overline{3}$ -structured compounds had been produced. Data were further analysed by Rietveld methods using the Bruker AXS software package *TOPAS*2.1 operated in the fundamental parameters mode (Kern & Coelho, 1998). Depending upon the presence of impurities the number of *TOPAS*2.1-refined variables ranged up to 45 independent parameters. These included: zero corrections; scaling factors; cell dimensions; atomic positional coordinates; preferred orientation corrections; crystal size and strain effects; isotropic thermal parameters. The occupation factors of all the sites were set to 1, except that of the mixed-occupation octahedral site A^{2+}, which was set in accordance with the initial mixture composition, as confirmed by SEM EDS.

The *ATOMS*6.0 software package (Dowty, 1999) was used to determine interaxial angles describing the distortion of the coordination polyhedra and selected bond lengths. The

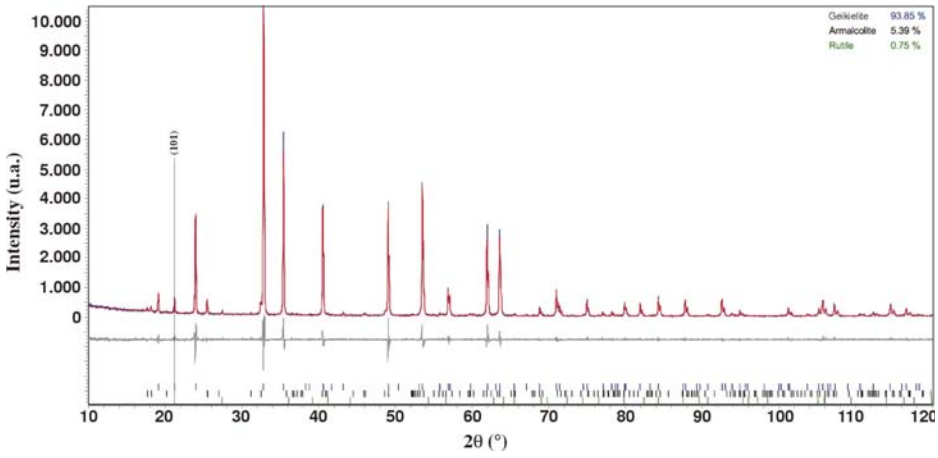

Figure 2
Rietveld refinement plot (line) of the X-ray powder diffraction data for $Mg_{0.7}Zn_{0.3}TiO_3$ at room temperature (dots). The vertical bar indicates the Bragg reflections which are allowed for the ordered ilmenite structure. The difference curves between observed and calculated profiles are plotted. For the agreement factors see Table 1.

*IVTON*2.0 program (Balić-Žunić & Vicković, 1996) was employed to characterize the coordination spheres of the cations, the volumes of the coordination polyhedra and the displacements of the cations from the centres of the coordination polyhedra.

3. Results

3.1. Synthetic zinc–manganese titanates

Our study has demonstrated that the synthesis of the $Mg_{1-x}Zn_xTiO_3$ ($0 \leq x \leq 0.8$) solid-solution series with increments of $x = 0.1$ a.p.f.u. Zn (atoms per formula unit) is possible at ambient pressure in air. However, $ZnTiO_3$ (ecandrewsite) and $Mg_{0.1}Zn_{0.9}TiO_3$ were not formed under our synthesis conditions in the temperature range 973–1573 K. The synthetic $MgTiO_3$ end-member, formed at a significantly higher temperature compared with the other compounds considered here, exhibits crystallochemical parameters (*see below*) which are considerably different from those of the compositionally similar $Mg_{0.9}Zn_{0.1}TiO_3$ and are similar to data published for synthetic $MgTiO_3$ (Wechler & von Dreele, 1989). Microprobe analyses show that all the titanates approach $A^{2+}TiO_3$ stoichiometry.

The X-ray powder diffraction patterns of all the $Mg_{1-x}Zn_xTiO_3$ compounds synthesized contain reflections with ($h0l$) (l = odd; see Fig. 2), resulting from the ordered distribution of A^{2+} and Ti^{4+} in alternate layers of the octahedra (Raymond & Wenk, 1971). These reflections are forbidden for the fully disordered corundum-type structure and $LiNbO_3$-type structure, and are not characteristic of either the armalcolite-like phase, $(Mg,Zn)Ti_2O_5$, or rutile which are present as minor (≤ 5 vol %) phases. These reflections became slightly diffuse for the titanate with $x = 0.8$ a.p.f.u. Zn (*see* below).

Some reflections of the armalcolite-like phase are very close to and overlap with those of the major reflections of the rhombohedral titanate. These overlaps include the (230), (240), (250) and (630) reflections of orthorhombic $(Mg,Zn)Ti_2O_5$, and the (104), (113), (024) and (030) reflections of rhombohedral $ATiO_3$ titanates. Nevertheless, the crystal structure parameters obtained for the armalcolite-bearing $MgTiO_3$ end-member (geikielite) are very close to those published by Wechsler & von Dreele (1989). We are confident that the accuracy of the determination of the crystallochemical parameters described here for other titanates was not affected by any overlap caused by minor phases.

For Rietveld refinement, we used the atomic coordinates given by Wechsler & von Dreele (1989) for synthetic $MgTiO_3$ as a starting model. Fig. 2 is a Rietveld refinement plot for synthetic $Mg_{0.7}Zn_{0.3}TiO_3$. The refinement and unit-cell parameters, polyhedra volumes, displacements (shifts) of $^{vi}A^{2+}$ and $^{vi}Ti^{4+}$ cations from the centers of coordination polyhedra, and parameters describing the distortion of coordination polyhedra (*see* below) in the synthesized titanates are summarized in Table 1. As expected, entry of the larger Zn^{2+} cation into the AO_6 site results in a regular increase in the unit-cell parameters and unit-cell volume with increasing Zn content (Fig. 3).

Atomic coordinates and isotropic thermal parameters are summarized in Table 2. Selected bond lengths and bond angles within and outside of the first coordination spheres of A and Ti atoms have been deposited.[1]

4. Crystal chemistry

We employed the Δ_n distortion index introduced by Shannon (1976) to illustrate polyhedron bond-length distortion, given as $\Delta_n = \frac{1}{n}\Sigma\{(r_i\bar{r})/\bar{r}\}^2 \times 10^3$, where r_i and $\bar{r}$ are individual and average bond lengths in the polyhedron, respectively. To characterize deviations from the ideal bond angles in regular octahedra, we calculate the bond-angle variance index, δ_n, where $\delta_n = \Sigma[(\theta_i - 90)^2/(n-1)]$, where θ_i are the bond angles at the central atom. The indices calculated and average bond lengths are given in Table 1.

As might be expected, the $\langle A{-}O\rangle$ distance increases with increasing x, whereas the $\langle Ti{-}O\rangle$ distance decreases (Table 1, Fig. 4). These changes result in an increase in the unit-cell volume and unit-cell dimensions through the series, in good

[1] Supplementary data for this paper are available from the IUCr electronic archives (Reference: TA5010). Services for accessing these data are described at the back of the journal.

Table 2
Atomic positions and isotropic displacement parameters (B_{iso}) of synthetic $(Mg_{1-x}Zn_x)TiO_3$ ($0 \leq x \leq 08$) at ambient conditions.

$A = {}^{vi}(Mn_{1-x}Zn_x)^{2+}$.

Position	Sample	x	y	z	B_{iso} (Å^2)
^{vi}A	$x = 0$	0	0	0.3573 (2)	0.19 (4)
	$x = 0.1$	0	0	0.3569 (2)	0.56 (4)
	$x = 0.2$	0	0	0.3578 (2)	0.51 (3)
	$x = 0.3$	0	0	0.3586 (2)	0.47 (4)
	$x = 0.4$	0	0	0.3596 (1)	0.59 (4)
	$x = 0.5$	0	0	0.3599 (1)	0.47 (4)
	$x = 0.6$	0	0	0.3602 (1)	0.58 (4)
	$x = 0.7$	0	0	0.3603 (1)	0.60 (4)
	$x = 0.8$	0	0	0.3602 (1)	0.95 (4)
^{vi}Ti	$x = 0$	0	0	0.1454 (1)	0.48 (3)
	$x = 0.1$	0	0	0.1451 (1)	0.43 (7)
	$x = 0.2$	0	0	0.1450 (1)	0.34 (2)
	$x = 0.3$	0	0	0.1452 (2)	0.24 (3)
	$x = 0.4$	0	0	0.1457 (1)	0.46 (4)
	$x = 0.5$	0	0	0.1459 (1)	0.54 (4)
	$x = 0.6$	0	0	0.1460 (1)	0.30 (4)
	$x = 0.7$	0	0	0.1460 (1)	0.31 (3)
	$x = 0.8$	0	0	0.1458 (1)	0.09 (4)
O1	$x = 0$	0.3174 (5)	0.0164 (6)	0.2485 (2)	1.05 (6)
	$x = 0.1$	0.3183 (5)	0.0217 (6)	0.2463 (2)	0.62 (5)
	$x = 0.2$	0.3173 (5)	0.0200 (7)	0.2460 (2)	0.58 (3)
	$x = 0.3$	0.3184 (5)	0.0211 (7)	0.2460 (2)	0.51 (5)
	$x = 0.4$	0.3196 (5)	0.0222 (7)	0.2460 (2)	0.80 (5)
	$x = 0.5$	0.3192 (5)	0.0214 (7)	0.2458 (2)	0.71 (4)
	$x = 0.6$	0.3176 (6)	0.0217 (8)	0.2454 (3)	0.49 (5)
	$x = 0.7$	0.3196 (5)	0.0238 (7)	0.2450 (4)	0.41 (5)
	$x = 0.8$	0.3214 (5)	0.0266 (6)	0.2435 (6)	0.36 (5)

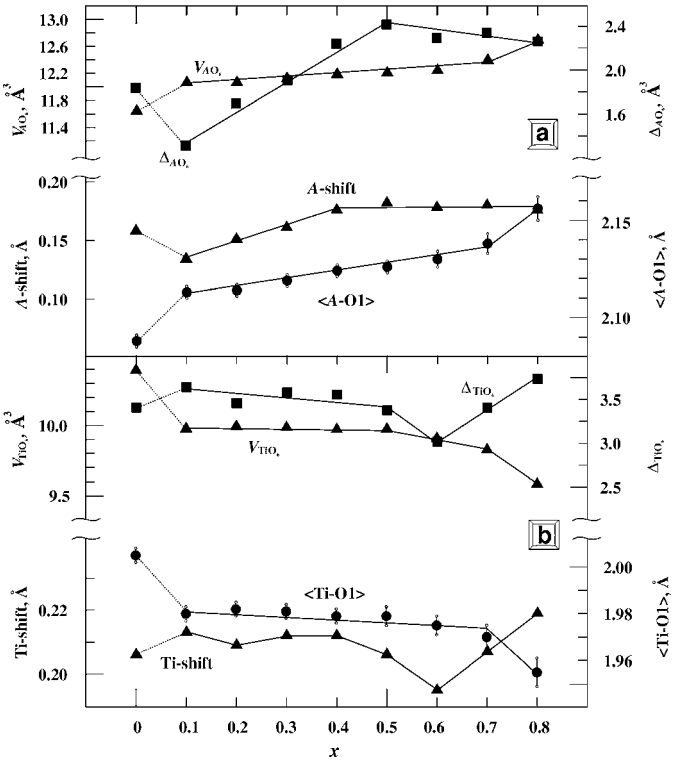

Figure 4
$Mg_{1-x}Zn_xTiO_3$ series: variations of the coordination polyhedra volumes, polyhedra distortion parameters (*see* text) and displacements of the A and Ti cations from the centers of the coordination polyhedra with the composition.

agreement with the entry of the larger Zn^{2+} cation into the layers of AO_6. As these are parallel to (001), this results in decreasing c/a ratios (Table 1, Fig. 3). Polyhedral volumes change antipathetically (Table 1, Fig. 4). Of note, the most Zn-rich titanate, $Mg_{0.2}Zn_{0.8}TiO_3$, exhibits an anomalously low TiO_6 volume and a high AO_6 volume (Table 1, Fig. 4). The

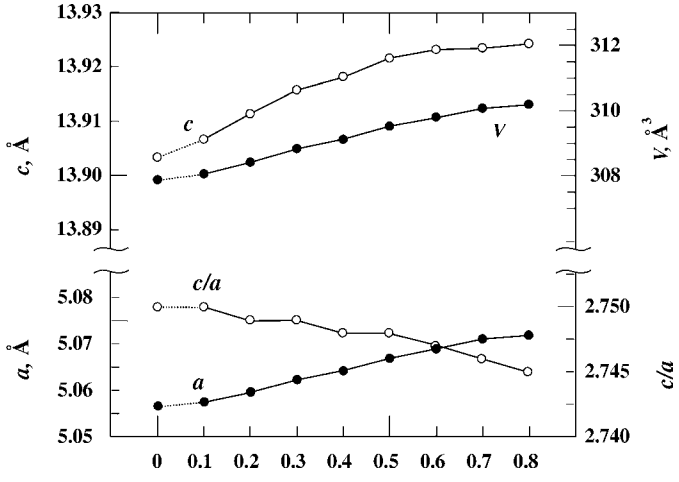

Figure 3
$Mg_{1-x}Zn_xTiO_3$ series: variations of the unit-cell parameters and volumes with composition. *Note*: the error bars are less than the dot size employed for plotting (Table 1).

AO_6 volume does not deviate from the trend found over the majority of the $Mg_{1-x}Zn_xTiO_3$ solid solution (x = 0.1–0.7 a.p.f.u. Zn; see Fig. 4*a*).

Throughout the series, the z coordinate of the A^{2+} cation does not change for compounds with x = 0.5–0.8, but increases for the compositional range of x = 0.1–0.4, deviating from 1/3; the z coordinate of the Ti cation varies very insignificantly with x (Fig. 4). Referring to the terminology of Wechsler & Prewitt (1984), these features infer that compositional changes drive the 'puckering' of the cation layers in Mg–Zn titanates only for AO_6 layers and only in the Mg-dominant titanates (*e.g.* zincian geikielite). This is not observed in their zincian analogs (magnesian ecandrewsite). The calculated displacement of the A^{2+} cations from the centers of the AO_6 coordination polyhedra shows a correlation with the changes in the $z_A{}^{2+}$ coordinate. Displacement of the Ti cations changes less regularly (Table 2, Fig. 4). Owing to the increased displacement of the A^{2+} cations, the layer consisting of AO_6 octahedra is more deformed compared with that composed of TiO_6 octahedra. The $A-A$ distance across the vacant octahedral site in the TiO_6 layer decreases slightly with the entry of the larger $^{vi}Zn^{2+}$ cation into the A site.[2]

The synthetic $Mg_{1-x}Zn_xTiO_3$ titanates consist of distorted coordination polyhedra similar to those occurring in $FeTiO_3$

[2] See footnote **1**.

and $MnTiO_3$ (Mitchell, 2002; Mitchell & Liferovich, 2004*b*). AO_6 octahedra exhibit less distortion than TiO_6 octahedra, as illustrated by the bond-length distortion indices (Table 1). The overall distortion of the AO_6 octahedra depends on the extent of Zn substitution in the range $x = 0.1$–0.5 and increases with increasing Zn; at $x \geq 0.5$ it remains high and varies insignificantly. Distortion of the TiO_6 octahedra is less dependent on the Zn $\leftrightarrow$ Mg diadochy and shows a minimum at $x = 0.6$, and increases with further increases in x. Bond-angle variance indices are less sensitive to the entry of $^{vi}Zn^{2+}$ into the A site and increase with x regularly. Bond-angle distortion in the TiO_6 octahedron varies less regularly (Table 1).

The overall trends of the crystallochemical characteristics in the series are complicated by the somewhat erratic parameters observed for the most Zn-rich titanates with $x = 0.6$–0.8 a.p.f.u. Zn (atoms per formula unit). Given the anomalously low volume of TiO_6 octahedra in these compounds (Fig. 4*b*), this anomaly cannot be due to the entry into this site of some Zn^{2+} and/or Mg^{2+} cations, which are larger than $^{vi}Ti^{4+}$ [0.74, 0.72 and 0.605 Å, respectively (Shannon, 1976)]. Refinement of the occupation of the ^{vi}Ti site by Rietveld methods does not indicate either divalent cations or any significant vacancies as $^{vi}SOF_{Ti}$ does not deviate from 1 a.p.f.u. Ti^{4+} within the accuracy of the methods for all titanates studied. As further increases in Zn content result in a collapse of the ilmenite structure to a mixture of spinel and rutile, we consider the compounds with $x = 0.6$–0.8 a.p.f.u. Zn to be metastable and most probably, partially disordered. The latter supposition is in agreement with the observation that the ($h0l$) (l = odd) reflections, allowed for ordered ABO_3 structures only, appear to be slightly diffuse for $Mg_{0.2}Zn_{0.8}TiO_3$, the member of the series with the most zinc content which is stable at ambient conditions. Note that the synthetic $Mn_{1-x}Zn_xTiO_3$ solid solution has also been recently found to be limited to $x = 0.8$ a.p.f.u. Zn (Mitchell & Liferovich, 2004*a*,*b*).

5. Conclusions

The experimentally obtained limit of solid solution between Zn and Mg in the structure of Fe-free $R\overline{3}$ titanates is *ca* 0.8 a.p.f.u. Zn. This value is identical to the limit obtained for $Mn_{1-x}Zn_xTiO_3$ solid-solution series and its naturally occurring compositional analogs (Mitchell & Liferovich, 2004*a*,*b*). The experimentally obtained upper limit of the Goldschmidt tolerance factors for $A^{2+}TiO_3$ titanates of the first-group transitional metals adopting ordered $R\overline{3}$ structures at ambient conditions is 0.755. Given the difference of the crystallographic characteristics of the high-temperature $MgTiO_3$ end-member from that of the $Mg_{0.9}Zn_{0.1}TiO_3$ compound, we conclude that the crystallographic parameters of the $R\overline{3}$ crystal structure are dependent on the kinetics of the synthesis. Doping of the MgO–TiO_2 system with as little as 0.1 a.p.f.u. Zn significantly broadens the stability field of the ordered $R\overline{3}$ titanates which are isostructural with ilmenite. The adoption of an $R\overline{3}$ structure by the $ZnTiO_3$ end-member composition at ambient conditions has not been confirmed by the present study, as this compound could not be synthesized. The data for ilmenite-structured zinc titanate currently listed in crystallographic databases requires re-evaluation.

This work was supported by the Natural Sciences and Engineering Research Council of Canada and Lakehead University (Canada). We are grateful to Allan MacKenzie for assistance with the analytical work and Anne Hammond for sample preparation. Constructive criticism provided by two reviewers and Dr M. R. Taylor is highly appreciated.

References

Balić-Žunić, T. & Vicković, I. (1996). *J. Appl. Cryst.* **29**, 305–306.
Bartram, S. F. & Slepetys, R. A. (1961). *J. Am. Ceram. Soc.* **44**, 493–499.
Birch, W. D., Burke, E. A. J., Wall, V. J. & Etheridge, M. A. (1988). *Mineral. Mag.* **52**, 237–240.
Dowty, E. (1999). *Atoms 5.0*. Shape Software, Kingsport, TN 37663, USA, http://shapesoftware.com.
Gatehouse, B. M. & Nesbit, M. C. (1978). Unpublished report. Department of Chemistry, Monash University (not seen; secondary reference from *Mineral. Mag.* **52**, 237–240, 1988).
Goldschmidt, V. M. (1926). *Skrifter Nor. Vidensk. Akad. Mat. Naturvidensk.* Kl., 2, 8, 194p.
Kern, A. A. & Coelho, A. A. (1998). *A New Fundamental Parameters Approach in Profile Analysis of Powder Data*, pp. 144–151. Bombay, India: Allied Publishers Ltd.
Kim, H. T., Kim, Yo., Valant, M. & Suvorov, D. (2001). *J. Am. Ceram. Soc.* **84**, 1081–1086.
Ko, J. & Prewitt, C. (1988). *Phys. Chem. Mineral.* **15**, 355–362.
Liferovich, R. P. & Mitchell, R. H. (2004). Accepted for publication.
Linton, J. A., Fei, Y. & Navrotsky, A. (1999). *Am. Mineral.* **84**, 1595–1603.
Mitchell, R. H. (2002). *Perovskites: Modern and Ancient.* Thunder Bay: Almaz Press; http://www.almazpress.com.
Mitchell, R. H. & Liferovich, R. P. (2004*a*). *Can. Mineral.* **42**, 1143–1152.
Mitchell, R. H. & Liferovich, R. P. (2004*b*). Accepted for publication.
Nakashima, K. & Imaoka, T. (1998). *Mineral. Petrol.* **63**, 1–17.
Plimer, I. R. (1990). *Neues Jahrb. Mineral. Monatsh.* **12**, 529–536.
Raymond, K. N. & Wenk, H. R. (1971). *Contrib. Mineral. Petrol.* **30**, 135–140.
Shannon, R. D. (1976). *Acta Cryst.* A**32**, 751–767.
Syono, Y., Akimoto, S., Ishikawa, Y. & Endoh, Y. (1969). *J. Phys. Chem. Solids*, **30**, 1665–1672.
Suwa, K., Enami, M., Hiraiwa, I. & Tang, T. (1987). *Mineral. Petrol.* **36**, 111–120.
Wechsler, B. A. & von Dreele, R. B. (1989). *Acta Cryst.* B**45**, 542–549.
Wechsler, B. A. & Prewitt, C. (1984). *Am. Mineral.* **69**, 176–185.
Whitney, D. L., Hirschmann, M. & Miller, M. G. (1993). *Can. Mineral.* **31**, 425–436.